Original Article

Defining lung adenocarcinoma subtypes with glucocorticoid-related genes and constructing a prognostic index for immunotherapy guidance

Hongguang Tang[1], Jianhua Zhu[1], Yongliang Wang[1], Jianjie Zhang[1], Jianwei Zhou[1], Zhoumiao Chen[2]

[1]Department of Thoracic Surgery, Xinchang Hospital of Wenzhou Medical University, Shaoxing, China; [2]Department of Thoracic Surgery, Sir Run Run Shaw Hospital, School of Medicine, Zhejiang University, Hangzhou, China

Contributions: (I) Conception and design: H Tang, J Zhu; (II) Administrative support: Y Wang, Z Chen; (III) Provision of study materials or patients: J Zhang, J Zhou; (IV) Collection and assembly of data: J Zhu, J Zhou, Z Chen; (V) Data analysis and interpretation: H Tang, Y Wang, J Zhang; (VI) Manuscript writing: All authors; (VII) Final approval of manuscript: All authors.

Correspondence to: Zhoumiao Chen, BSc. Department of Thoracic Surgery, Sir Run Run Shaw Hospital, School of Medicine, Zhejiang University, 3 Qingchun East Road, Shangcheng District, Hangzhou 310016, China. Email: czhoumiao@163.com.

Background: Several studies have shown that glucocorticoid-related genes (GCGs) play a crucial role in cancer. However, the mechanism of GCGs in lung adenocarcinoma (LUAD) is not fully understood. This study aimed to identify distinct subtypes of LUAD by integrating GCGs and to develop prognostic models for precise prognosis prediction and immunotherapy guidance.

Methods: In this study, sample data of LUAD were collected from The Cancer Genome Atlas (TCGA) database, and unsupervised clustering was used to identify LUAD subtypes with different GCGs characteristics. Survival-related genes were screened by differential expression analysis and protein-protein interaction (PPI) network analysis. After that, the least absolute shrinkage and selection operator (LASSO) combined with Cox regression analysis was used to establish the prognosis model. Differences in the immune microenvironment of different risk groups were analyzed, and Tumor Immune Dysfunction and Exclusion (TIDE) was used to predict the response of patients to immunotherapy. Finally, the CellMiner database was used to predict potential drugs.

Results: Two subtypes of LUAD were identified, namely cluster 1 (high survival rate) and cluster 2 (low survival rate). A prognostic model was constructed based on 9 characteristic genes, including *CLCA1*, *CYP17A1*, *GRIA2*, *IGFBP1*, *IGF2BP1*, *NTSR1*, *RPE65*, *VGF*, and *WNT16*, and the prognosis of LUAD patients was positively predicted. There were differences in the immune microenvironment of different risk LUAD patients, and high-risk LUAD patients may benefit less from immunotherapy. BGB-283 was a candidate for LUAD targeting VGF.

Conclusions: Our study elucidates the impact of GCGs on LUAD prognosis and immune responses, offering insights for prognostic forecasting and immunotherapeutic strategies for LUAD patients.

Keywords: Glucocorticoid-related genes (GCGs); immunotherapy; lung adenocarcinoma (LUAD); prognostic models; subtypes

Submitted Jul 09, 2024. Accepted for publication Jan 10, 2025. Published online Apr 28, 2025. This article was updated on October 27, 2025.

The original version was available at: https://dx.doi.org/10.21037/jtd-24-1083

doi: 10.21037/jtd-24-1083

Introduction

Globally, lung cancer poses a significant threat as a malignant tumor (1), with lung adenocarcinoma (LUAD) patients enduring a distressing 5-year survival rate below 15% due to late-stage diagnosis (2,3). Tumor heterogeneity within and across LUAD cases presents a substantial diagnostic obstacle, complicating treatment success (4).

While the classification based on tissue features helps tailor LUAD treatments, it falls short in unraveling the complexities of LUAD pathogenesis and treatment decisions (5). Hence, there is a pressing need to delve into the mechanisms of LUAD tumorigenesis, identify effective biomarkers, and pinpoint potential therapeutic targets for more precise prognostic forecasts.

Glucocorticoids (GCs), a class of corticosteroids within the steroid hormone family, have been extensively utilized in oncology support and palliative care (6). Notably, in LUAD, studies have highlighted the impact of GC medicines like dexamethasone (DEX) (7) and prednisolone (8) on manipulating LUAD cell proliferation through various molecular pathways. The activation of the glucocorticoid receptor (GR) by GCs has been associated with inducing dormancy in lung cancer cells, thus impeding proliferation (9). This underscores the potentially pivotal role of GCs in LUAD onset and progression, yet the exploration of GCs-associated prognostic genes in LUAD is still replete with many unknowns.

Our study utilized unsupervised clustering analysis to categorize LUAD subtypes based on distinct glucocorticoid-related gene (GCG) characteristics. By scrutinizing subtype gene interactions, we identified candidate genes linked to prognosis and devised a potential LUAD prognostic model. Delving into signaling pathways, immune microenvironments, and gene mutation frequencies among high- and low-risk LUAD patient cohorts could provide valuable insights for tailoring immunotherapy strategies. The prospect of targeting signature genes with drugs opens new avenues for therapeutic research. Overall, this study expands our knowledge of GCGs in LUAD, offering insights into prognostic evaluation and further study of immunotherapy in LUAD patients. We present this article in accordance with the TRIPOD reporting checklist (available at https://jtd.amegroups.com/article/view/10.21037/jtd-24-1083/rc).

Highlight box

Key findings

- A prognostic risk model based on glucocorticoid-related genes (GCGs) was constructed.

What is known and what is new?

- According to GCGs, lung adenocarcinoma (LUAD) patients can be divided into two subtypes with significant survival differences.
- There were significant differences in the immune microenvironment among different risk groups, and patients in the high-risk group had a poorer response to immunotherapy.

What is the implication, and what should change now?

- Additional prognostic markers have been identified for LUAD patients, but further experimental validation of the results is needed.

Methods

Data acquisition

A total of 59 normal and 541 LUAD samples (including gene expression profiles and clinical data such as age, gender, tumor grade, and tumor node metastasis (TNM) staging) were sourced from The Cancer Genome Atlas (TCGA) database (https://portal.gdc.cancer.gov/). The validation set was sourced from the GSE50081 dataset at Gene Expression Omnibus (GEO) (https://www.ncbi.nlm.nih.gov/). From GeneCards (https://www.genecards.org/), 783 GCGs were obtained, filtered by a relevance score above 2. The study was conducted in accordance with the Declaration of Helsinki and its subsequent amendments.

Identification of LUAD subtypes associated with GCGs characteristics

Through univariate Cox regression analysis, we identified GCGs that correlate with LUAD patient survival in the training set. Then, according to the expression level of GCGs, we used the *ConsensusClusterPlus* R package to determine the optimal cluster number and conducted 1,000 repetitions to ensure the classification stability. The survival status differences between LUAD subtypes post-clustering were analyzed to gauge the classification efficacy of GCGs.

Construction and validation of LUAD prognostic model

The *edgeR* R package was applied for differential analysis to identify differentially expressed genes (DEGs) between LUAD subtypes cluster 1 and cluster 2 [false discovery rate (FDR) <0.05, logFC >1]. A protein-protein interaction (PPI) network for the DEGs was created using the Search Tool for the Retrieval of Interacting Genes/Proteins (STRING) database, where only interactions with a confidence score of ≥0.7 were included. Further, univariate Cox regression analysis was used to screen for genes that were significantly associated with LUAD survival. Least absolute shrinkage and selection operator (LASSO) penalization from the

glmnet R package was employed to streamline the list of survival-related genes, with parameter λ optimized by 10-fold cross-validation. The *survminer* R package then performed multivariate Cox regression analysis on the Lasso-selected genes to construct the definitive LUAD prognostic model. Patients were divided into high- and low-risk groups based on the median risk score. The distribution of risk scores, survival status, and the expression differences of characteristic genes across the risk groups were illustrated. The Kaplan-Meier survival curve assessed the disparity in survival rates between the groups. The GSE50081 samples served as a validation cohort to further substantiate its prognostic validity. The R package *timeROC* was used to generate receiver operating characteristic (ROC) curves and calculate the area under the curve (AUC) values to further evaluate the predictive efficacy of the prognostic model.

Construction and validation of a prognostic nomogram

To confirm the capability of the model's risk scores in forecasting LUAD prognosis, we conducted univariate and multivariate Cox regression analyses on clinical attributes of LUAD patients, including age, gender, TNM, and stage, as well as the risk scores. The clinical factors identified by the prognostic model and multivariate Cox regression analysis were then integrated, using the R package *rms* to build a nomogram to predict 1-, 2-, and 3-year overall survival. Decision curve analysis (DCA) curves were drawn to evaluate the effectiveness of the nomogram. ROC curves were plotted to evaluate the clinical potential of the model. Calibration curves were used to assess the deviation between the nomogram and the actual value (1, 2, and 3 years).

Detection and enrichment analysis of DEGs

With the *edgeR* R package, differential expression analysis was carried out on the high- and low-risk groups from the training set to identify DEGs (FDR <0.05, logFC >1). Gene Ontology (GO) and Kyoto Encyclopedia of Genes and Genomes (KEGG) enrichment analysis for these DEGs was conducted using the *clusterProfiler* R package to explore their biological functions. The enrichment results were graphically presented using the *enrichplot* R package.

Immune microenvironment analysis

The single sample gene set enrichment analysis (ssGSEA) method guided us to conduct a differential analysis of immune cell infiltration and immune-related functions between risk groups employing the gene set variation analysis (GSVA) R package. The expression levels of human leukocyte antigen (HLA) related genes and immune checkpoint molecules were statistically compared between the groups. The Tumor Immune Dysfunction and Exclusion (TIDE) algorithm was applied to assess the sensitivity of LUAD patients with different risk levels to immunotherapy. The results were visualized by violin plots following Wilcoxon testing.

Tumor mutation analysis

The *maftools* R package was used to analyze and compare the mutation, status, types, single nucleotide variant (SNV) classes, and mutation rates in the high- and low-risk groups of LUAD patients, based on SNV mutation data from TCGA, and to visualize the top 20 mutated genes in a gene waterfall plot.

Drug prediction

The *CellMiner* database (https://discover.nci.nih.gov/cellminer/home.do) was employed to forecast potential drugs that may act on the genes of the prognostic model, applying the half maximal inhibitory concentration (IC_{50}) as the gauge for drug sensitivity.

Statistical analysis

All statistical analyses were performed using R (version 4.0.2; http://www.r-project.org/about.html). Pearson correlation coefficient was used to study the correlation between risk score and immune infiltration level, immunotherapy response, and TIDE score. Univariate Cox regression analysis, multivariate Cox regression analysis, and LASSO regression analysis were used to screen model genes. Kaplan-Meier analysis was used to assess the association between risk scores and survival. ROC curves were used to verify the predictive efficiency of the model. $P<0.05$ was considered to indicate a statistically significant difference.

Results

Identification and survival analysis of LUAD subtypes

From 783 GCGs, 118 genes were identified as significantly

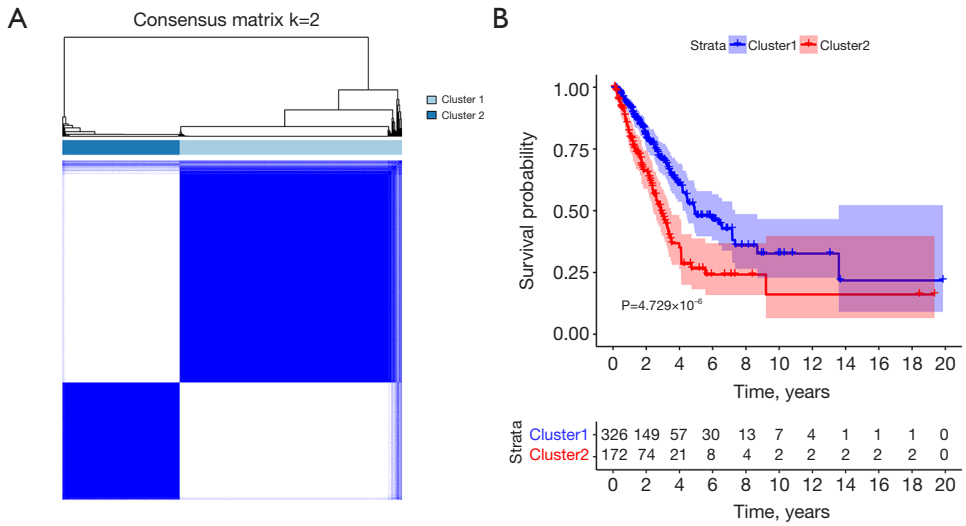

Figure 1 Identification of LUAD subtypes and evaluation of the typing ability of GCGs. (A) LUAD clustering results based on GCG expression; (B) survival analysis of the two subtypes after clustering. GCGs, glucocorticoids-related genes; LUAD, lung adenocarcinoma.

associated with LUAD prognosis via univariate Cox regression analysis (table available at https://cdn.amegroups.cn/static/public/jtd-24-1083-1.xlsx). Subsequently, unsupervised clustering based on GCG expression among LUAD samples led to two subtypes, cluster 1 (n=326) and cluster 2 (n=172) (*Figure 1A*). The survival analysis showed a significant divergence in survival status between these two subtypes (P=4.729×10^{-6}) (*Figure 1B*), with a higher survival rate observed in cluster 1. This demonstrated the validity of GCG-based LUAD subtype classification for subsequent research.

Assessment of prognostic model predictive capacity

Differential expression analysis of the cluster 1 and cluster 2 subtypes led to the discovery of 403 DEGs (table available at https://cdn.amegroups.cn/static/public/jtd-24-1083-2.xlsx). A PPI network was then constructed (number of nodes: 401, number of edges: 223, average node degree: 1.11, avg. local clustering coefficient: 0.279, expected number of edges: 41, PPI enrichment P value: <1.0e−16), where 159 DEGs were found to interact (*Figure 2*, table available at https://cdn.amegroups.cn/static/public/jtd-24-1083-3.xlsx). These genes were to be considered for the prognostic model. Following univariate Cox regression analysis and tuning of the Lasso coefficient with parameter λ, 17 genes associated with LUAD survival were identified (*Figure 3A,3B*). A prognostic model with 9 genes was then established through multivariate Cox regression (*Figure 3C*). The model formula is as follows:

$$\begin{aligned} Riskscore = & -0.149281745*CLCA1 - 0.137673074*CYP17A1 \\ & - 0.087378951*GRIA2 + 0.05675468*IGF2BP1 \\ & + 0.081689231*IGFBP1 + 0.048219114*NTSR1 \\ & + 0.125469274*RPE65 + 0.095176458*VGF \\ & - 0.101370953*WNT16 \end{aligned} \quad [1]$$

Our research posited a strong correlation between the nine characteristic genes and the prognosis of LUAD. By evaluating the expression levels of these genes, we ascertained the prognostic risks for LUAD patients within the training cohort, subsequently stratifying them into high- and low-risk groups (*Figure 4A*). An assessment of the survival status within these risk groups indicated a higher mortality rate for the high-risk group (*Figure 4B*). Furthermore, the expression patterns of the prognostic genes exhibit marked variations between the two groups (*Figure 4C*). Employing Kaplan-Meier survival analysis, we concluded that the survival rate for the high-risk group was notably lower than that of the low-risk group (P=5.946×10^{-10}) (*Figure 4D*). To determine the validity of the prognostic model, we generated ROC curves for 1, 3, and 5 years, obtaining AUC values of 0.74, 0.74, and 0.72, respectively, all above 0.7 (*Figure 4E*). This suggests that the model has a robust predictive capacity for LUAD prognosis. Moreover, we further tested its accuracy using the GSE50081 validation set. The validation set mirrored the training set in terms of survival status and

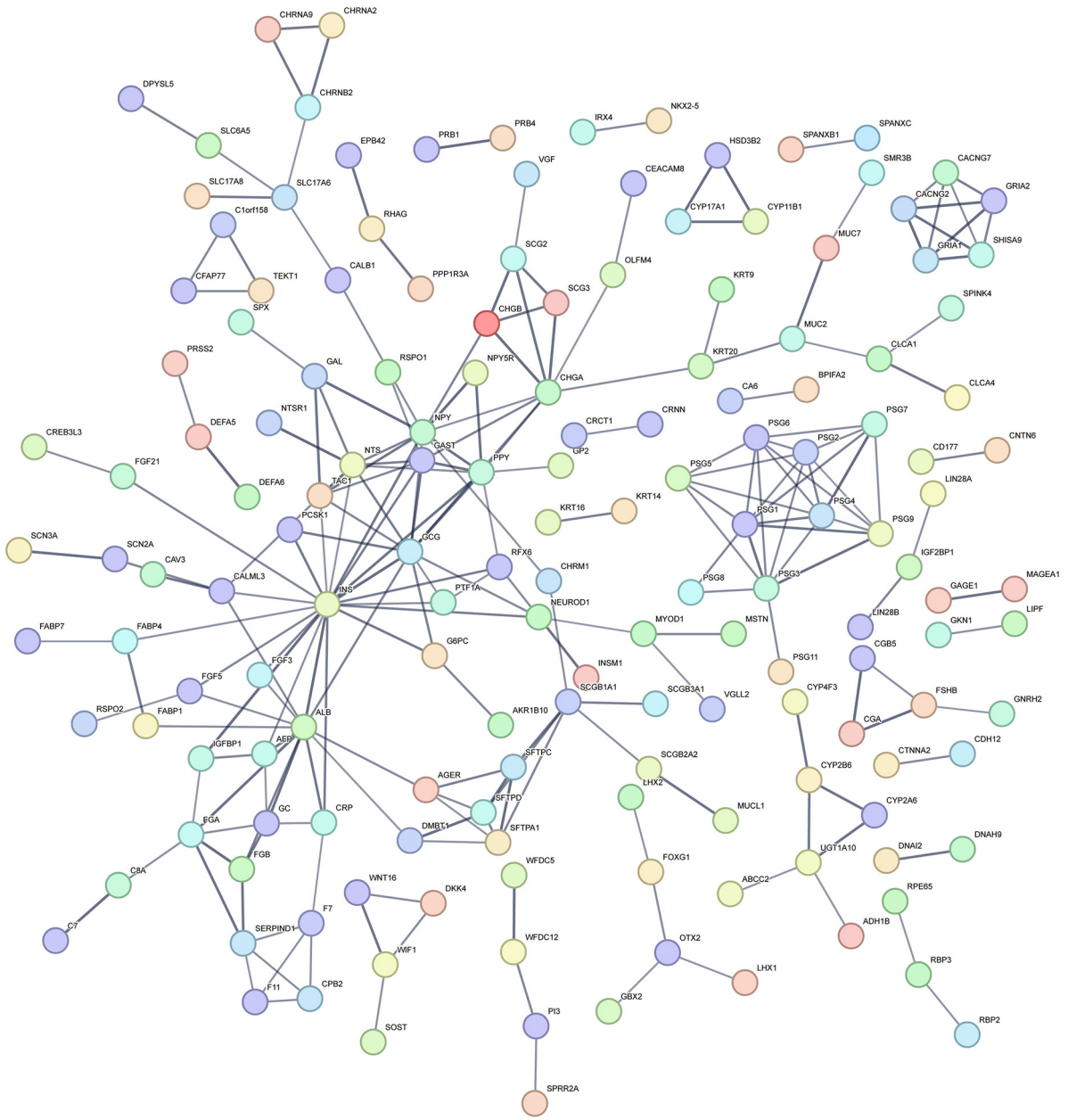

Figure 2 PPI network of 159 DEGs in clusters 1 and 2. DEGs, differentially expressed genes; PPI, protein-protein interaction.

the characteristic gene expression of the high- and low-risk groups (*Figure 4F-4H*). The Kaplan-Meier survival curve demonstrated that the survival rate in the high-risk group is still significantly lower ($P=1.64\times10^{-4}$) (*Figure 4I*). The ROC curves displayed AUC values of 0.71, 0.71, and 0.76 for 1, 3, and 5 years, respectively, indicating the excellent forecasting ability of the prognostic model (*Figure 4J*). In conclusion, the model, performing superior forecasting for LUAD prognosis, can be utilized in further research.

Independent prognosis value of the risk score in the prognostic model

To verify whether the risk score could independently foretell the prognosis of LUAD patients, we employed

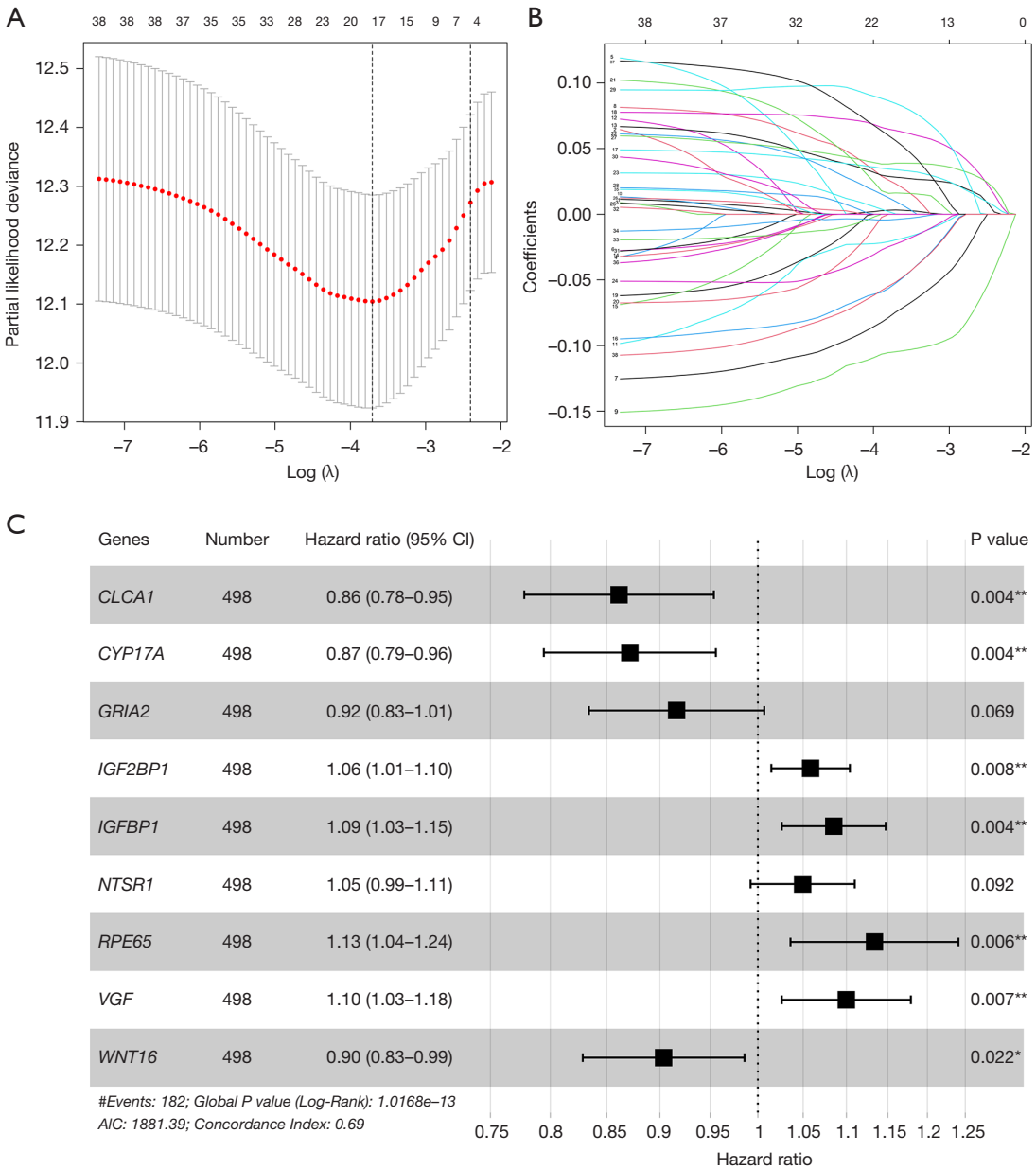

Figure 3 Construction of the prognostic model for LUAD. (A) Coefficient distribution chart from ten-fold cross-validation for the LASSO model, with λ as the tuning parameter; (B) LASSO coefficient curve; (C) forest plot from the multivariate Cox regression analysis. *, P<0.05; **, P<0.01. AIC, Akaike information criterion; CI, confidence interval; LASSO, least absolute shrinkage and selection operator; LUAD, lung adenocarcinoma.

univariate and multivariate Cox regression analyses to assess the clinical features and risk scores of LUAD samples (*Figure 5A*,*5B*). The findings indicated that the risk score is an independent predictor of LUAD patient prognosis (P<0.001). Then we developed a nomogram from the prognostic model to project the 1-, 2-, and 3-year clinical outcomes for LUAD patients (*Figure 5C*). Calibration curve analysis showed a strong correlation between the predicted and actual survival rates (*Figure 5D*). suggesting that our nomogram precisely predicted LUAD patient survival rates. The ROC curves revealed the highest AUC value for the risk score, at 0.764 (*Figure 5E*), indicating its superior

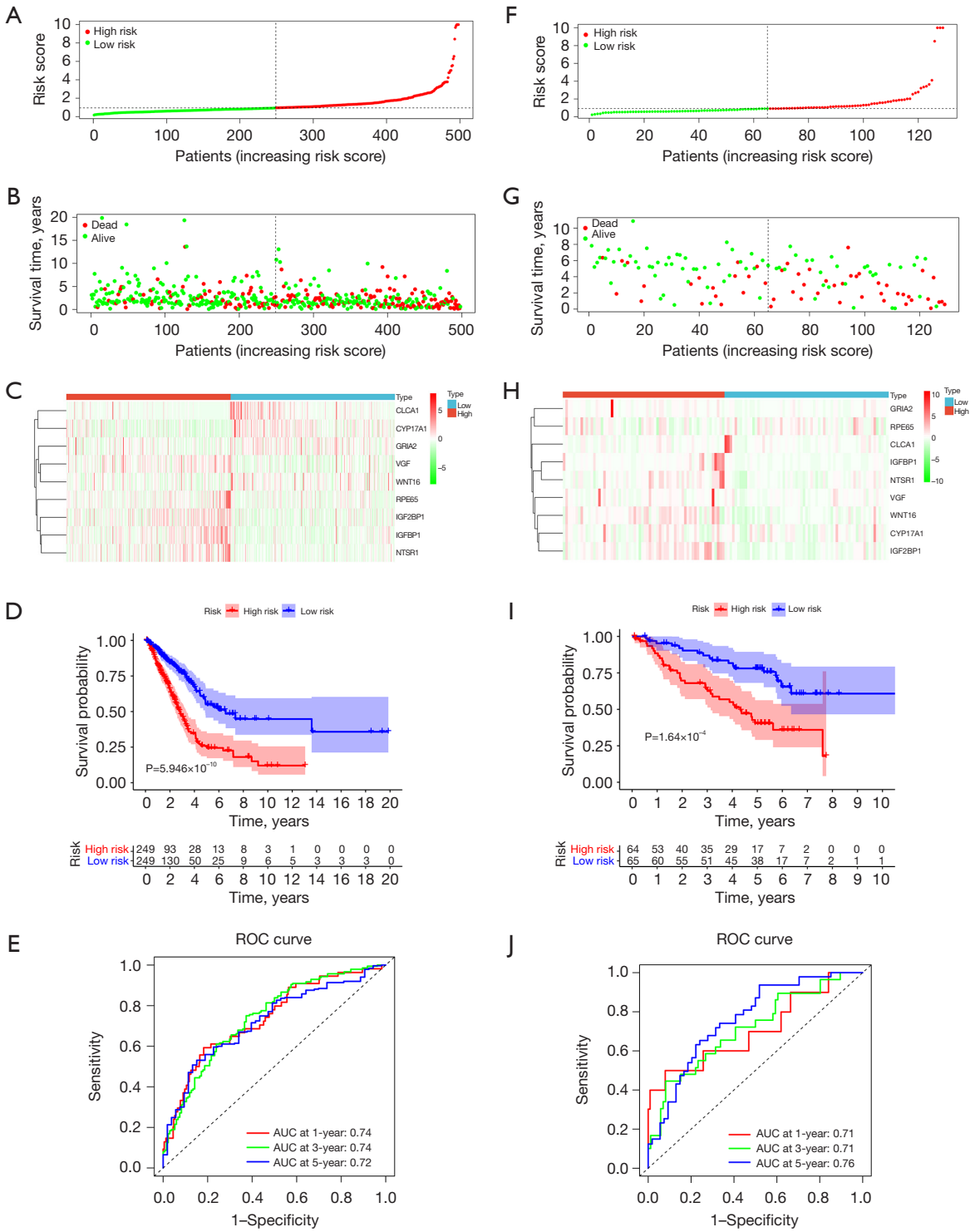

Figure 4 Evaluation and validation of LUAD prognostic model. (A) Risk score distribution, (B) survival conditions, (C) characteristic gene expression, (D) survival curves, and (E) ROC curves for the high- and low-risk groups in the TCGA training cohort. (F) Risk score distribution, (G) survival conditions, (H) characteristic gene expression, (I) survival curves, and (J) ROC curves for the high- and low-risk groups in the GSE50081 validation cohort. AUC, area under the curve; LUAD, lung adenocarcinoma; ROC, receiver operating characteristic; TCGA, The Cancer Genome Atlas.

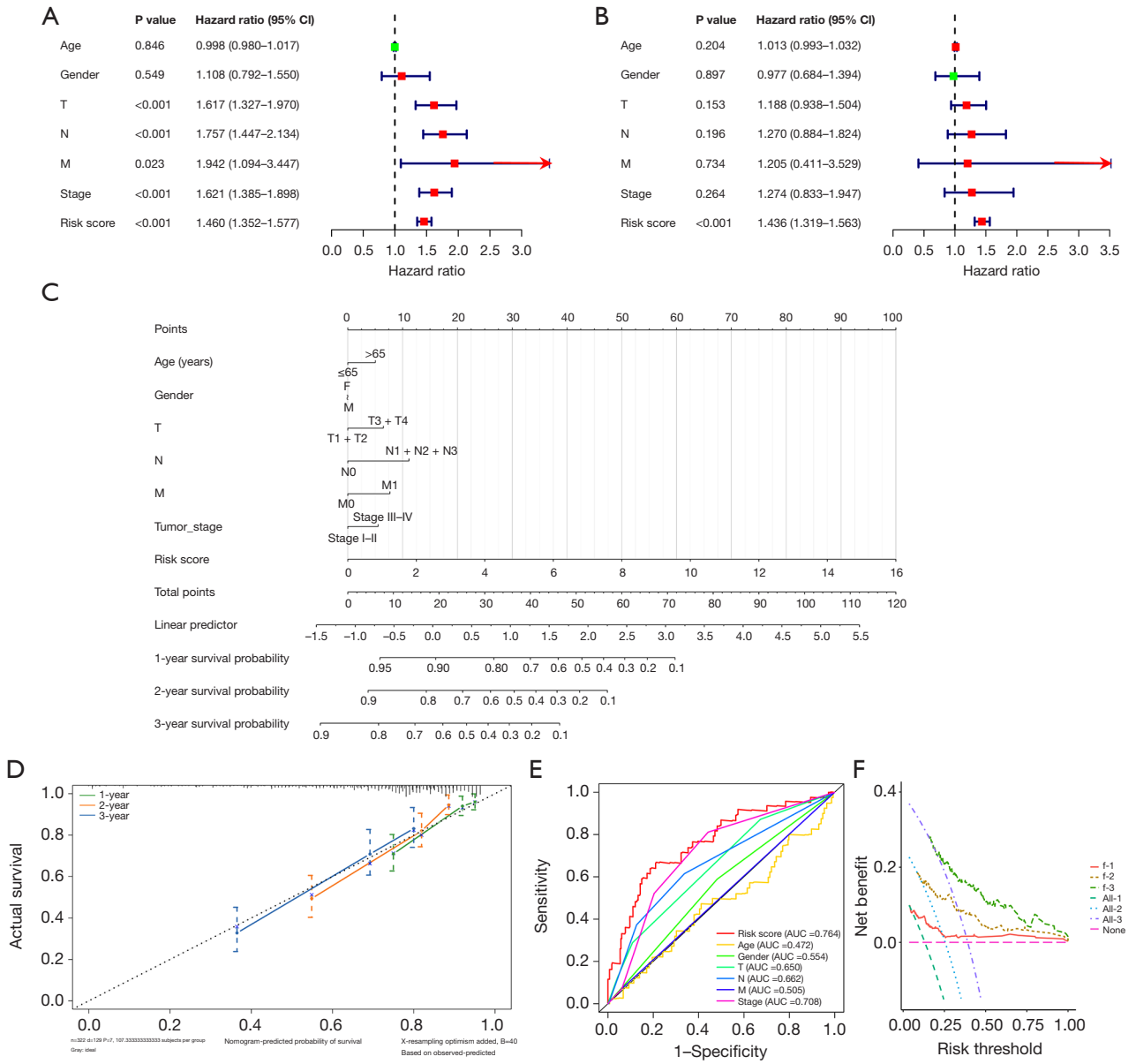

Figure 5 The independent prediction of the prognostic model. (A) Forest plot from univariate Cox regression analysis with combined clinical features and risk scores. (B) Forest plot from multivariate Cox regression analysis with integrated clinical features and risk scores. (C) Nomogram created based on clinical features and risk scores. (D) Calibration plots for 1-, 2-, and 3-year predictions by the nomogram. (E) ROC curves for the assessment of clinical features and the risk score. (F) DCA curves for the nomograms at 1, 2, and 3 years. AUC, area under the curve; CI, confidence interval; DCA, decision curve analysis; ROC, receiver operating characteristic.

prognostic performance in comparison to other clinical characteristics. The DCA curves suggested that the model may perform well in clinical practice (*Figure 5F*). These findings support the idea that the 9 genes in the prognostic model can act as independent prognostic factors for LUAD patients.

Examination of the underlying biological functions in LUAD patients with different risk levels

A differential expression analysis was executed between the risk groups, culminating in the identification of 1,129 DEGs (table available at https://cdn.amegroups.cn/static/public/

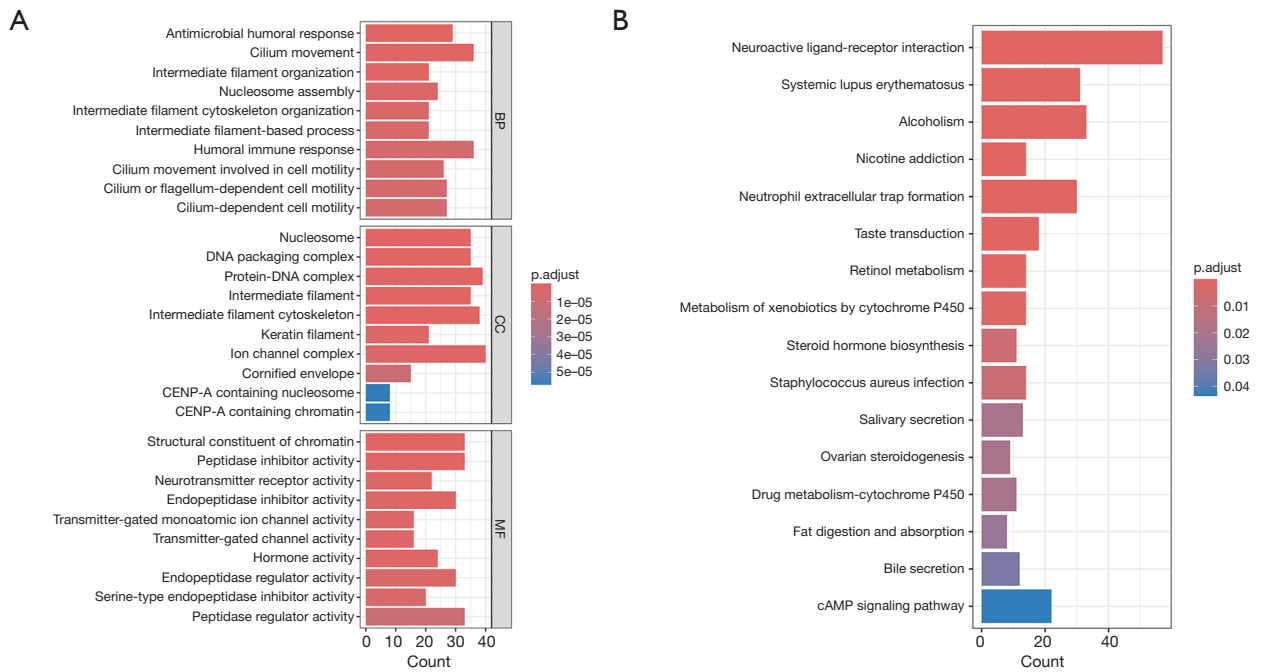

Figure 6 Examination of the underlying biological functions in LUAD patients in different risk groups. (A) GO enrichment plot for DEGs between the high- and low-risk groups. (B) KEGG enrichment plot for DEGs between the high- and low-risk groups. BP, biological process; cAMP, cyclic adenosine monophosphate; CC, cellular component; DEGs, differentially expressed genes; GO, Gene Ontology; LUAD, lung adenocarcinoma; MF, molecular function; KEGG, Kyoto Encyclopedia of Genes and Genomes.

jtd-24-1083-4.xlsx). An enrichment analysis of DEGs was performed to elucidate the variances in signaling pathways between two risk cohorts. GO enrichment analysis showed that these DEGs were mainly concentrated in GO entries such as cilium-dependent cell motility, ion channel complex, structural constituent of chromatin, and neurotransmitter receptor activity (*Figure 6A*). Similarly, KEGG enrichment analysis showed that DEGs are mainly associated with pathways like neuroactive ligand-receptor interaction, systemic lupus erythematosus, neutrophil extracellular trap formation, and cyclic adenosine monophosphate (cAMP) signaling pathway (*Figure 6B*). These findings imply that the DEGs within the high- and low-risk groups predominantly participate in biological processes related to cell signaling and metabolism.

Immune profiling in LUAD patients with varying risk values

Using ssGSEA, we found a marked divergence in the immunological profiles between the high- and low-risk patient cohorts. Specifically, the high-risk cohort demonstrated an elevated presence of Tfh (P=0.002) and Th1 cells (P=0.04), contrasting with a diminished presence of aDCs ($P=2.56\times10^{-8}$), iDCs (P=0.001), mast cells ($P=1.55\times10^{-4}$), and neutrophils ($P=3.27\times10^{-4}$) (*Figure 7A*). Concurrently, there was a discernible variation in the enrichment of immunological pathways, with the high-risk group exhibiting increased expression in functions such as APC_co_stimulation (P=0.02), MHC_class_I ($P=8.18\times10^{-5}$), parainflammation (P=0.003), and Inflammation.promoting (P=0.002), and decreased expression in HLA (P=0.003) and Type_II_IFN_Response ($P=6.79\times10^{-4}$) (*Figure 7B*). The statistical profiles of HLA-related gene expression further backed up the findings. Specifically, the genes *HLA-A* (P=0.03) and *HLA-G* (P=0.002) demonstrated elevated expression within the high-risk cohort, while the genes *HLA-DMA* (P=0.003), *HLA-DMB* (P=0.003), *HLA-DOA* (P=0.003), *HLA-DOB* (P=0.02), *HLA-DPA1* (P=0.02), *HLA-DPB1* (P=0.02), *HLA-DQB2* (P=0.001), *HLA-DRA* (P=0.02), and *HLA-DRB5* (P=0.002) were highly expressed in the low-risk cohort (*Figure 7C*). Subsequent analysis of immune checkpoints showed a pronounced upregulation of *LAG3* (P=0.003),

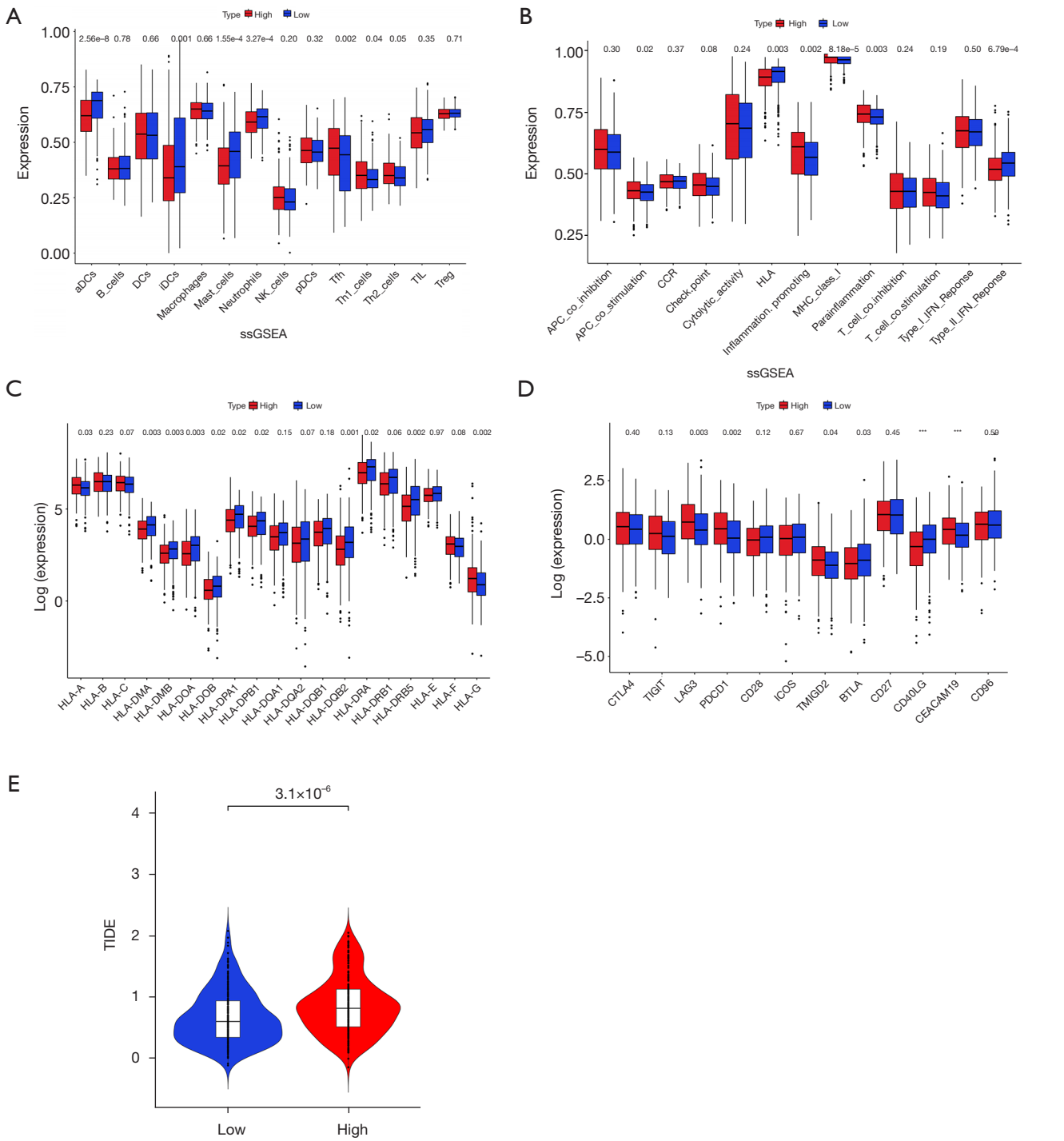

Figure 7 Immune profiling in LUAD patients with varying risk values. (A) Infiltration levels of immune cells in both risk groups. (B) Expression levels of immune cell functions in both risk groups. (C) Expression of HLA-related genes in both risk groups. (D) Expression of immune checkpoints in the high- and low-risk groups. (E) TIDE scores between the high- and low-risk groups. ***, P<0.001. aDCs, activated dendritic cells; APC, antigen-presenting cell; CCR, C-C chemokine receptor; iDCs, immature dendritic cells; MHC, major histocompatibility complex; NK, natural killer cells; IFN, interferon; HLA, human leukocyte antigen; LUAD, lung adenocarcinoma; pDCs, plasmacytoid dendritic cells; ssGSEA, single sample gene set enrichment analysis; TIDE, Tumor Immune Dysfunction and Exclusion; TIL, tumor-infiltrating lymphocytes.

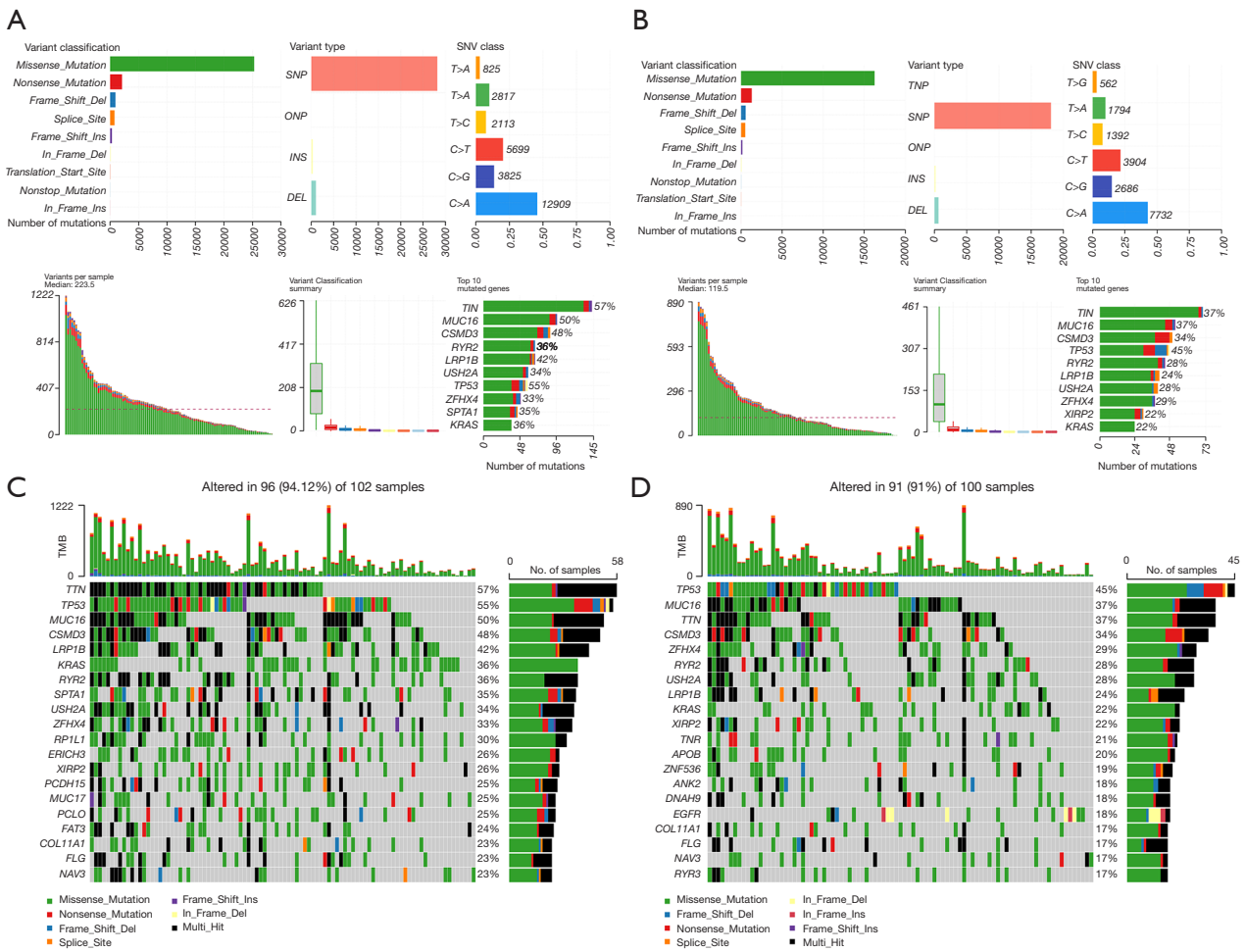

Figure 8 Mutation profiling in high- and low-risk LUAD patient groups. (A,B) A statistical overview of mutation types and their distribution in the (A) high-risk and (B) low-risk groups. (C,D) Top 20 mutation types and their prevalence in the (C) high-risk and (D) low-risk groups. LUAD, lung adenocarcinoma.

PDCD1 (P=0.002), *TMIGD2* (P=0.04), and *CEACAM19* (P=4.90×10^{-3}) in the high-risk cohort, and conversely, *BTLA* (P=0.03) and *CD40LG* (P=2.72×10^{-4}) exhibited increased expression within the low-risk cohort (*Figure 7D*). Potential divergence in immunotherapy responsiveness was revealed. The TIDE algorithm also helped us uncover a higher immune evasion rate in the high-risk group (P<0.001) (*Figure 7E*). Overall, these results suggested the need for tailored immunotherapy for LUAD patients with varying risk levels.

Mutation profiling

We investigated genetic mutation variances between high- and low-risk groups via maftools R, identifying Missense_Mutations as the most frequent in both groups, with a cytosine(C)-to-adenine(A) transition trend in SNV nucleotide sites (*Figure 8A,8B*). The top 20 mutated genes were congruent between risk groups (*Figure 8C,8D*). Notably, *TTN* exhibited the highest mutation frequency in the high-risk group at 57%, while *TP53* showed a mutation rate of 45%, which was the highest in the low-risk group. These mutation rate variances might be responsible for the varying risk profiles in LUAD patients.

Potential drug prediction

We used CellMiner database to pinpoint drugs for prognostic gene markers. The gene *VGF* showed the highest drug sensitivity. Thus, we spotlighted the top nine drugs

that exhibited a significant positive correlation with the *VGF* gene (P<0.001), namely Dabrafenib (Cor =0.641), ARQ-680 (Cor =0.621), PLX-4720 (Cor =0.614), Vemurafenib (Cor =0.604), BGB-283 (Cor =0.576), PLX-8394 (Cor =0.573), MLN-2480 (Cor =0.572), TAK-632 (Cor =0.569), and GDC-0994 (Cor =0.549) (*Figure 9A*). Further, we compared the drug sensitivity in the high and low expression groups of *VGF*, with the measure IC_{50}. BGB-283 demonstrated the most pronounced difference in IC_{50} values between the high and low *VGF* expression groups (P<0.05) (*Figure 9B*). Overall, BGB-283 emerges as a candidate drug for *VGF*-targeted LUAD therapy.

Discussion

The potent heterogeneity of LUAD leads to its intricate pathogenic mechanisms. Classification of LUAD based on histological features has facilitated the development

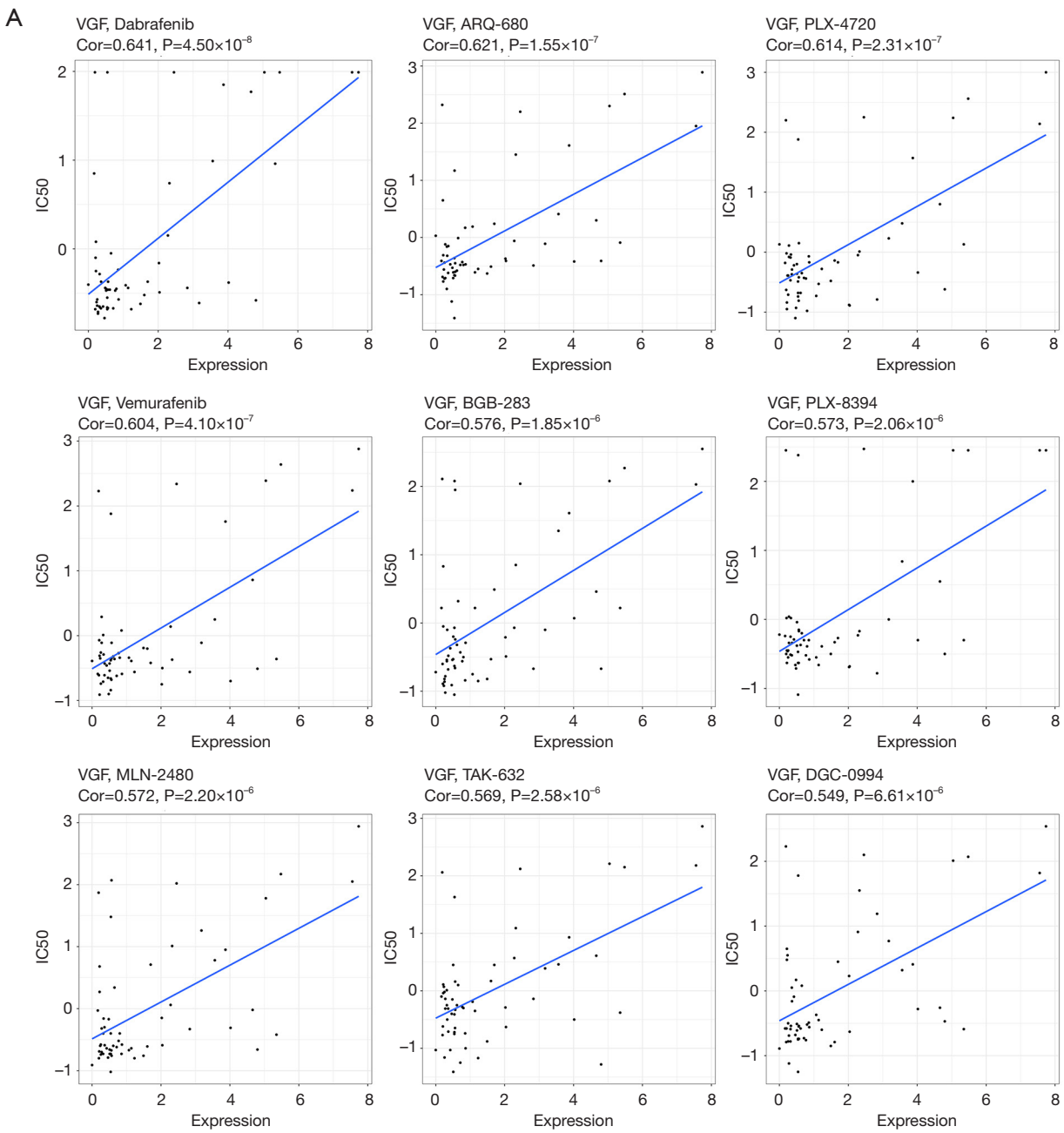

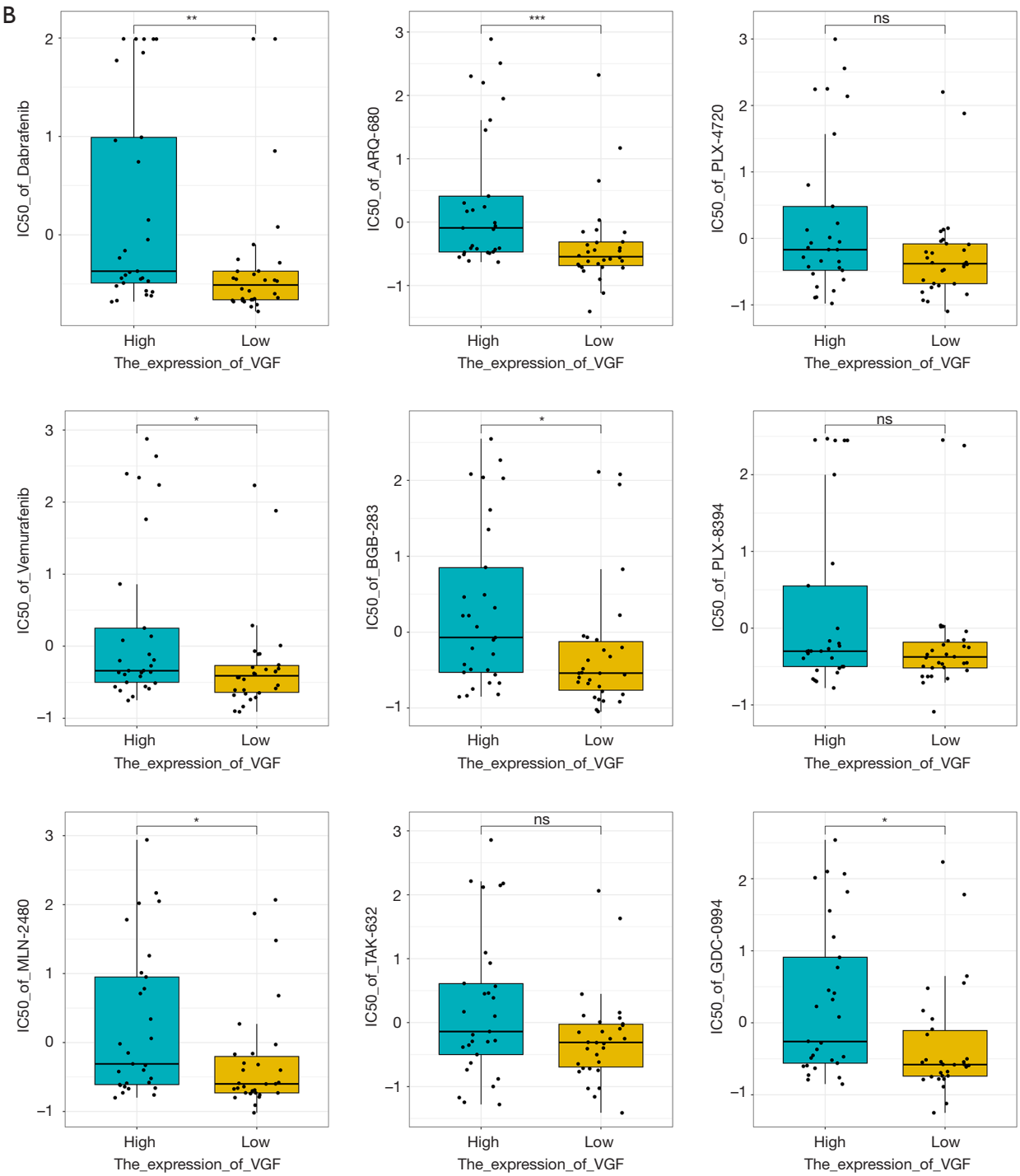

Figure 9 Prediction of potential drugs targeting the gene *VGF*. (A) Sensitivity analysis of the top 9 drugs targeting the gene *VGF*. (B) IC50 values of the 9 drugs in high and low expression groups of *VGF*. ns, P>0.05; *, P<0.05; **, P<0.01; ***, P<0.001. *VGF*, nerve growth factor inducible; IC50, inhibitory concentration.

of targeted treatment strategies, yet the prognostic prediction of LUAD is still elusive (10-12), necessitating further refinement. The synergy between GCs and their receptors is a key regulatory mechanism for the body's ecological balance, with the lung's normal maturation being intrinsically tied to the GCs-GR axis (13,14). Previous research also highlighted the role of the GCs-GR axis in the progression of lung cancer and its resistance to treatment. Sasaki *et al.* have uncovered the involvement of GCs and GR pathway in LUAD recurrence and prognosis, and also identified the downstream regulatory genes, NDRG-1, and the protein kinase SGK-1, as key prognostic factors for LUAD (15). These insights point to a strong correlation between the GCs-GR pathway and LUAD, potentially aiding in LUAD prognostic research.

This research, based on the expression of GCGs, grouped LUAD patients into two prognostic subtypes—cluster 1 (higher survival rates) and cluster 2 (lower survival rates), thereby highlighting the prognostic significance of the GR in LUAD. Following a differential analysis of these subtypes, we developed a prognostic model, revealing an association between LUAD prognosis and 9 specific genes: *CLCA1*, *CYP17A1*, *GRIA2*, *IGFBP1*, *IGF2BP1*, *NTSR1*, *RPE65*, *VGF*, and *WNT16*. Notably, *CLCA1*, identified as a secreted autolytic protein, modulates calcium-dependent chloride channels, thereby implicating itself in cellular processes such as proliferation, migration, and metastasis (16). Studies have substantiated the modulatory role of TMEM16A, a calcium-gated chloride channel protein, in tumorigenesis and invasiveness of lung cancer cells, with *CLCA1* identified as a direct modulatory agent of TMEM16A (17,18). The study of *CLCA1* in lung cancer remains unexplored, offering a promising avenue for future research into LUAD pathogenesis and development. *CYP17A1*, a versatile hydroxylase within the cytochrome P450 enzyme family, primarily governs the biosynthesis of sex hormones, thereby influencing neoplastic conditions such as prostate and breast cancer (19,20). Zhang *et al.* (21) identified *CYP17A1* as a potential candidate gene for non-small cell lung cancer (NSCLC) susceptibility. However, its polymorphism showed no association with NSCLC development in Asian populations. Recent findings suggest that low *CYP17A1* expression in high-risk LUAD cohorts acts as a protective factor (22), aligning with the outcomes of this investigation. *GRIA2*, encoding a subunit of the AMPA-type ionotropic glutamate receptors, is recognized as a neurotransmitter receptor reliant on lung and breast cancer cells (23). *IGFBP1*, a potent regulator of insulin-like growth factor (IGF) activity, influences cancer progression by modulating essential cellular processes such as proliferation, migration, invasion, and apoptosis (24). Elevated *IGFBP1* levels have been linked to poorer LUAD prognosis (25). *In vivo* and *in vitro* experimental data demonstrate that *IGFBP1* suppression inhibits LUAD cell proliferation, migration, and epithelial-mesenchymal transition (EMT) capabilities, suppressing tumor growth (26). Cai *et al.* (27) demonstrated that *IGFBP1* maintains cancer cell survival and drives tumor metastasis by regulating the phosphorylation and activity of *SOD2* in lung cancer. *NTSR1*, a G protein-coupled receptor, participates in neurotransmission and metabolic processes through its interaction with neurotensin peptides (28). As upregulated in LUAD, *NTSR1* stimulates EMT and cell metastasis through the Wnt/β-catenin pathway (29). Recently, Chen *et al.* (30) elucidated that *NTSR1* facilitates the migration and invasiveness of pulmonary oncocytes via the reconfiguration of the cytoskeletal architecture. *RPE65*, an enzyme with retinol isomerase activity, catalyzes the conversion of all-trans-retinyl esters to 11-cis-retinol (31). Limited studies have addressed the role of *RPE65* in lung cancer. In a comprehensive pan-cancer analysis, Keshavarz-Rahaghi *et al.* (32) identified *RPE65* as a genetic trait linked to the loss of p53 function. More recently, Zhou *et al.* (33) highlighted RPE65 as a potential prognostic indicator for LUAD by examining crucial smoking-related genes in LUAD, correlating it with poorer outcomes. Hence, in conjunction with our findings, *RPE65* emerges as a novel marker for LUAD, yet further experimental validation remains imperative. VGF, as a neurotrophic factor, is involved in the regulation of EGFR-TKI resistance in LUAD (34,35). Li *et al.* (36) uncovered through bioinformatics that VGF serves as a standalone prognostic indicator in forecasting the overall survival of NSCLC patients. Additionally, Shi *et al.* (37) demonstrated that *METTL3* enhances the malignancy of LUAD cells by controlling VGF through transcriptional regulation (histone modification) and post-transcriptional modification (m6A). *WNT16* is a member of the WNT ligand family, and the abnormal expression of WNT ligands plays a crucial role in the etiology and progression of various malignancies, inclusive of NSCLC and colorectal cancer (38,39). In summary, the nine identified GCGs in this study likely contribute to LUAD onset and progression, potentially serving as biomarkers. However, further experimental investigations are crucial to

elucidate the specific roles of these genes in LUAD.

A novel modality in oncology by stimulating the human immune system, immunotherapy marks a breakthrough in the therapeutics of LUAD (40). In this context, we investigated the potential therapeutic benefits of immunotherapy among LUAD patients stratified by risk. Analysis of immune cell infiltration profiles revealed elevated expression of Th1 cells within the high-risk cohort, in contrast to augmented expression of aDCs and iDCs within the low-risk cohort. It is well-documented that T cells are the primary targets in the immunotherapy of lung cancer (41). Th1 cells, a subset of T cells, are known to secrete tumor necrosis factor (TNF)-α, interleukin (IL)-2, and interferon-gamma (IFN-γ), cytokines that are instrumental in mounting an effective anti-tumor immune response (42). Contrary to this, Ito *et al.* (43) observed in tumor-infiltrating lymphocytes (TIL) of lung cancer patients that Th1 cells were less effective in producing IFN-γ, suggesting a potential suppression of Th1 cell function in the context of lung malignancies. Dendritic cells (DCs), endowed with exceptional antigen-presenting efficacy, are capable of eliciting antigen-specific T cell reactions and thus rendered as pivotal vaccine targets in lung cancer immunotherapy (44), which comes as a pleasant relief for low-risk LUAD population. Advanced research has uncovered remarkable variations in the immune functional profiles across LUAD patients with diverse risk stratifications. Pulmonary inflammation, instigated by an array of stressors including smoking and particulates, is a contributing factor in the genesis of lung cancer, and Kraemer *et al.* have discerned a marked decrement in the cytotoxic T cell infiltration within lung cancer specimens with heightened inflammation scores (45,46). Meanwhile, inflammatory episodes are known to induce the upregulation of major histocompatibility complex (MHC) class I within pulmonary epithelial cells, thereby augmenting the immunosurveillance against malignant lung cells (47), elucidating why there existed heightened expression of immune functions such as Inflammation. promoting, MHC class I, and parainflammation in high-risk LUAD patients with lower survival rates. Immune evasion is a defining characteristic of cancer. It has been established that the attenuation of HLA allele expression may precipitate a reduction in antigen presentation, encouraging the immune evasion and metastatic dissemination of lung cancer (48,49). Thus, the pronounced expression of numerous HLA genes in the low-risk group might curtail the immune evasive mechanisms of pulmonary oncogenic genes. The TIDE algorithmic assessment corroborated this proposition. Intriguingly, the high-risk group persists in the heightened expression of *HLA-A* and *HLA-G* genes, potentially accounting for the marked variance in immune checkpoint expression between the groups. In essence, this prognostic model may inform the immunotherapeutic strategies for LUAD.

We further explored the genetic mutation profiles across the risk cohorts, uncovering notable similarities between them. Utilizing the CellMiner database to predict drugs targeting the signature gene *VGF*, we ventured that BGB-283 is a promising candidate for LUAD therapeutics. Yet, the mechanism of action of the drug and its treatment effects require further investigation.

Conclusions

Collectively, our research harnessed bioinformatics to discern two LUAD subtypes characterized by distinct GCGs, clusters 1 and 2, and subsequently developed a robust LUAD prognostic model predicated on the divergences among these subtypes. This model holds immense value in guiding LUAD immunotherapy. Targeting specific genes and pathways can enhance treatment outcomes for LUAD patients. By utilizing predictive models, we can evaluate risk scores for early screening and monitoring of high-risk groups. Notably, our findings suggest that patients in the low-risk category are more responsive to immune therapy. Therefore, the implementation of a risk assessment model by our research institute can aid in tailoring personalized treatment decisions for LUAD, improving clinical management. Furthermore, customizing immunotherapy and medication selection can boost medical service efficiency and quality, minimizing resource waste and lowering treatment costs. Yet, there are limitations to this study that warrant attention: (I) the study is limited by a restricted sample pool and did not include biological experiments to confirm the accuracy of LUAD subtype predictions and classifications. (II) The exact molecular mechanisms by which GCGs regulate LUAD are not delineated, which will be the primary focus in our next phase of research.

Acknowledgments

None.

Footnote

Reporting Checklist: The authors have completed the TRIPOD reporting checklist. Available at https://jtd.amegroups.com/article/view/10.21037/jtd-24-1083/rc

Peer Review File: Available at https://jtd.amegroups.com/article/view/10.21037/jtd-24-1083/prf

Funding: None.

Conflicts of Interest: All authors have completed the ICMJE uniform disclosure form (available at https://jtd.amegroups.com/article/view/10.21037/jtd-24-1083/coif). The authors have no conflicts of interest to declare.

Ethical Statement: The authors are accountable for all aspects of the work in ensuring that questions related to the accuracy or integrity of any part of the work are appropriately investigated and resolved. The study was conducted in accordance with the Declaration of Helsinki and its subsequent amendments.

References

1. Kratzer TB, Bandi P, Freedman ND, et al. Lung cancer statistics, 2023. Cancer 2024;130:1330-48.
2. Reck M, Remon J, Hellmann MD. First-Line Immunotherapy for Non-Small-Cell Lung Cancer. J Clin Oncol 2022;40:586-97.
3. Seguin L, Durandy M, Feral CC. Lung Adenocarcinoma Tumor Origin: A Guide for Personalized Medicine. Cancers (Basel) 2022;14:1759.
4. de Sousa VML, Carvalho L. Heterogeneity in Lung Cancer. Pathobiology 2018;85:96-107.
5. Willner J, Narula N, Moreira AL. Updates on lung adenocarcinoma: invasive size, grading and STAS. Histopathology 2024;84:6-17.
6. Denaro N, Garrone O, Morelli A, et al. A narrative review of the principal glucocorticoids employed in cancer. Semin Oncol 2022;49:429-38.
7. Xu M, Wang X. Critical roles of mucin-1 in sensitivity of lung cancer cells to tumor necrosis factor-alpha and dexamethasone. Cell Biol Toxicol 2017;33:361-71.
8. Choi HS, Kim SL, Kim JH, et al. The FDA-Approved Anti-Asthma Medicine Ciclesonide Inhibits Lung Cancer Stem Cells through Hedgehog Signaling-Mediated SOX2 Regulation. Int J Mol Sci 2020;21:1014.
9. Prekovic S, Schuurman K, Mayayo-Peralta I, et al. Glucocorticoid receptor triggers a reversible drug-tolerant dormancy state with acquired therapeutic vulnerabilities in lung cancer. Nat Commun 2021;12:4360.
10. Mäkinen JM, Laitakari K, Johnson S, et al. Histological features of malignancy correlate with growth patterns and patient outcome in lung adenocarcinoma. Histopathology 2017;71:425-36.
11. Travis WD, Brambilla E, Geisinger KR. Histological grading in lung cancer: one system for all or separate systems for each histological type? Eur Respir J 2016;47:720-3.
12. Li R, Li Z, Yang Z, et al. The presence of micropapillary and/or solid subtypes is an independent prognostic factor for patients undergoing curative resection for stage I lung adenocarcinoma with ground-glass opacity. Transl Lung Cancer Res 2024;13:256-68.
13. Cohen DM, Steger DJ. Nuclear Receptor Function through Genomics: Lessons from the Glucocorticoid Receptor. Trends Endocrinol Metab 2017;28:531-40.
14. Bird AD, McDougall AR, Seow B, et al. Glucocorticoid regulation of lung development: lessons learned from conditional GR knockout mice. Mol Endocrinol 2015;29:158-71.
15. Sasaki T, Nakamura Y, Hata S, et al. The GR-SGK1-NDRG1 Pathway as a Predictor of Recurrence and Prognosis in Lung Adenocarcinoma After Radical Surgery. Anticancer Res 2023;43:2965-74.
16. Liu CL, Shi GP. Calcium-activated chloride channel regulator 1 (CLCA1): More than a regulator of chloride transport and mucus production. World Allergy Organ J 2019;12:100077.
17. Jia L, Liu W, Guan L, et al. Inhibition of Calcium-Activated Chloride Channel ANO1/TMEM16A Suppresses Tumor Growth and Invasion in Human Lung Cancer. PLoS One 2015;10:e0136584.
18. Sala-Rabanal M, Yurtsever Z, Nichols CG, et al. Secreted CLCA1 modulates TMEM16A to activate Ca(2+)-

dependent chloride currents in human cells. Elife 2015;4:e05875.
19. Gomez L, Kovac JR, Lamb DJ. CYP17A1 inhibitors in castration-resistant prostate cancer. Steroids 2015;95:80-7.
20. Wróbel TM, Jørgensen FS, Pandey AV, et al. Non-steroidal CYP17A1 Inhibitors: Discovery and Assessment. J Med Chem 2023;66:6542-66.
21. Zhang Y, Hua S, Zhang A, et al. Association between polymorphisms in COMT, PLCH1, and CYP17A1, and non-small-cell lung cancer risk in Chinese nonsmokers. Clin Lung Cancer 2013;14:45-9.
22. Wu Y, Fu L, Wang B, et al. Construction of a prognostic risk assessment model for lung adenocarcinoma based on Integrin β family-related genes. J Clin Lab Anal 2022;36:e24419.
23. Deshpande K, Martirosian V, Nakamura BN, et al. Neuronal exposure induces neurotransmitter signaling and synaptic mediators in tumors early in brain metastasis. Neuro Oncol 2022;24:914-24.
24. Lin YW, Weng XF, Huang BL, et al. IGFBP-1 in cancer: expression, molecular mechanisms, and potential clinical implications. Am J Transl Res 2021;13:813-32.
25. Yao Z, Han J, Wu J, et al. Deciphering the multidimensional impact of IGFBP1 expression on cancer prognosis, genetic alterations, and cellular functionality: A comprehensive Pan-cancer analysis. Heliyon 2024;10:e37402.
26. Li Y, Yang X, Han T, et al. IGFBP1 promotes the proliferation and migration of lung adenocarcinoma cells through the PPARα pathway. Transl Oncol 2024;49:102095.
27. Cai G, Qi Y, Wei P, et al. IGFBP1 Sustains Cell Survival during Spatially-Confined Migration and Promotes Tumor Metastasis. Adv Sci (Weinh) 2023;10:e2206540.
28. Iyer MR, Kunos G. Therapeutic approaches targeting the neurotensin receptors. Expert Opin Ther Pat 2021;31:361-86.
29. Zhang Z, Zhang D, Su K, et al. NTSR1 promotes epithelial-mesenchymal transition and metastasis in lung adenocarcinoma through the Wnt/β-catenin pathway. Mutat Res 2024;829:111877.
30. Chen YL, Liu YN, Lin YT, et al. LncRNA SLCO4A1-AS1 suppresses lung cancer progression by sequestering the TOX4-NTSR1 signaling axis. J Biomed Sci 2023;30:80.
31. Kiser PD. Retinal pigment epithelium 65 kDa protein (RPE65): An update. Prog Retin Eye Res 2022;88:101013.
32. Keshavarz-Rahaghi F, Pleasance E, Kolisnik T, et al. A p53 transcriptional signature in primary and metastatic cancers derived using machine learning. Front Genet 2022;13:987238.
33. Zhou D, Sun Y, Jia Y, et al. Bioinformatics and functional analyses of key genes in smoking-associated lung adenocarcinoma. Oncol Lett 2019;18:3613-22.
34. Yang LH, Lee RK, Kuo MH, et al. Neuronal survival factor VGF promotes chemoresistance and predicts poor prognosis in lung cancers with neuroendocrine feature. Int J Cancer 2022;151:1611-25.
35. Hwang W, Chiu YF, Kuo MH, et al. Expression of Neuroendocrine Factor VGF in Lung Cancer Cells Confers Resistance to EGFR Kinase Inhibitors and Triggers Epithelial-to-Mesenchymal Transition. Cancer Res 2017;77:3013-26.
36. Li R, Liu X, Zhou XJ, et al. Identification and validation of the prognostic value of immune-related genes in non-small cell lung cancer. Am J Transl Res 2020;12:5844-65.
37. Shi K, Sa R, Dou L, et al. METTL3 exerts synergistic effects on m6A methylation and histone modification to regulate the function of VGF in lung adenocarcinoma. Clin Epigenetics 2023;15:153.
38. Xue W, Cai L, Li S, et al. WNT ligands in non-small cell lung cancer: from pathogenesis to clinical practice. Discov Oncol 2023;14:136.
39. Bugter JM, Fenderico N, Maurice MM. Publisher Correction: Mutations and mechanisms of WNT pathway tumour suppressors in cancer. Nat Rev Cancer 2021;21:64.
40. Lahiri A, Maji A, Potdar PD, et al. Lung cancer immunotherapy: progress, pitfalls, and promises. Mol Cancer 2023;22:40.
41. Wu Y, Yuan M, Wang C, et al. T lymphocyte cell: A pivotal player in lung cancer. Front Immunol 2023;14:1102778.
42. Mateu-Jimenez M, Curull V, Pijuan L, et al. Systemic and Tumor Th1 and Th2 Inflammatory Profile and Macrophages in Lung Cancer: Influence of Underlying Chronic Respiratory Disease. J Thorac Oncol 2017;12:235-48.
43. Ito N, Nakamura H, Metsugi H, et al. Dissociation between T helper type 1 and type 2 differentiation and cytokine production in tumor-infiltrating lymphocytes in patients with lung cancer. Surg Today 2001;31:390-4.
44. Lee JM, Lee MH, Garon E, et al. Phase I Trial of Intratumoral Injection of CCL21 Gene-Modified Dendritic Cells in Lung Cancer Elicits Tumor-Specific Immune Responses and CD8(+) T-cell Infiltration. Clin Cancer Res 2017;23:4556-68.
45. Kraemer AI, Chong C, Huber F, et al. The immunopeptidome landscape associated with T cell

infiltration, inflammation and immune editing in lung cancer. Nat Cancer 2023;4:608-28.
46. Miron O, Afrasanie VA, Paduraru MI, et al. The relationship between chronic lung diseases and lung cancer - a narrative review. J BUON 2020;25:1687-92.
47. Mathé J, Benhammadi M, Kobayashi KS, et al. Regulation of MHC Class I Expression in Lung Epithelial Cells during Inflammation. J Immunol 2022;208:1021-33.
48. Ivanova M, Shivarov V. HLA genotyping meets response to immune checkpoint inhibitors prediction: A story just started. Int J Immunogenet 2021;48:193-200.
49. McGranahan N, Rosenthal R, Hiley CT, et al. Allele-Specific HLA Loss and Immune Escape in Lung Cancer Evolution. Cell 2017;171:1259-1271.e11.

Cite this article as: Tang H, Zhu J, Wang Y, Zhang J, Zhou J, Chen Z. Defining lung adenocarcinoma subtypes with glucocorticoid-related genes and constructing a prognostic index for immunotherapy guidance. J Thorac Dis 2025;17(4):1888-1905. doi: 10.21037/jtd-24-1083